Journal of Nematology 22(3):362–385. 1990.

Ultrastructure of Phasmid Development in *Meloidodera floridensis* and *M. charis* (Heteroderinae)[1]

L. K. CARTA[2] AND J. G. BALDWIN[3]

Abstract: Phylogenetic characters for Heteroderinae Luc. et al., 1988 are evaluated in *Meloidodera* which is believed to have primarily ancestral characters. Phasmid ultrastructure is observed in second-stage juveniles (J2), third-stage juvenile males, fourth-stage juvenile males, and fifth-stage males of *Meloidodera floridensis* and *M. charis*. Phasmid secretion occurs inside the egg before the J1–J2 molt. Before J2 hatch, concentric lamellar membranes occur within the sheath and socket cells. Some membranes become lamellae of the sheath cell plasma membrane; others become multilamellar bodies. During early molting, plasma membrane lamellae disappear and a distal dendrite segment appears in a rudimentary canal. After the molt, the distal dendrite is not present within the canal. The phylogenetic utility of phasmid features is discussed. In both species the ampulla shape and size between molts are stable features in juveniles and males. The posthatch J2 sheath cell receptor cavity may vary in a species specific manner, but comparative morphology requires precise timing after hatch.

Key words: end apparatus, Heteroderinae, male development, *Meloidodera floridensis*, *Meloidodera charis*, molting, multilamellar body, neuromorphology, phasmid, phylogeny, secretion, ultrastructure.

Phasmid sensory organs have useful taxonomic characters in many secernentean nematodes (42) including the Heteroderinae Luc et al., 1988 (Heteroderidae sensu lato) (30). In a cladistic analysis of the Heteroderinae, a question arose about the structure of the phasmid. Although the character states of the phasmid opening had an apparent phylogenetic polarity of lens shape to pore shape, one species with a pore had been grouped with otherwise similar species having a lens (14,15). This problem was resolved when it was demonstrated with transmission electron microscopy (TEM) that the so-called pore-shaped phasmid opening of *Meloidodera charis* Hopper, 1960 was really a lens similar to, but smaller than, that of *M. floridensis* Chitwood et al., 1956 (2). The range of variability needs to be completely understood if phasmid characters are to be used in an updated phylogenetic analysis. There have been insufficient reliable characters to determine a phylogenetic pattern for the Heteroderinae, which contains numerous new genera (2,3).

A few free-living, animal-parasitic and plant-parasitic nematode phasmids have been examined at the ultrastructural level (1,5,9,31,33,44,47). Phasmids have a cuticle-lined opening that may be differentiated into an ampulla, which is usually occluded by a plug of electron-dense material (Fig. 1). The ampulla leads to a narrow cuticular canal contained within one or two socket cells which are developmentally derived from the hypodermis and are connected to the hypodermis and the basal region of the sheath cell by intercellular junctions. These junctions have been described as tight junctions or belt desmosomes (38). The socket cells also surround portions of the sheath cell. The sheath cell secretes an electron-dense substance within its extracellular receptor cavity which loosely surrounds the distal ends of one or two ciliary dendrites. From the sheath cell receptor cavity, the dendrites pass anteriorly within the tightly surrounding arms of sheath cell cytoplasm; they are delineated from the cytoplasm by intercellular junctions. The distal region of the neuron

Received for publication 4 August 1988.

[1] This research was supported in part by the National Science Foundation grant BSR-84-15627 and represents a part of the first author's Ph.D. dissertation. Mention of a product or trade name does not constitute an endorsement of that product.

[2] Research Fellow, Division of Biology, California Institute of Technology, Pasadena, CA 91125.

[3] Associate Professor, Department of Nematology, University of California, Riverside, CA 92521.

The authors thank D. T. Kaplan, USDA, Orlando, Florida, for supplying cultures of *Meloidodera floridensis*, H. T. Simte, University of California, Riverside, for technical assistance with one of the many tested fixation procedures, and M. A. McClure, University of Arizona, Tucson, for access to unpublished research on *Meloidodera charis*.

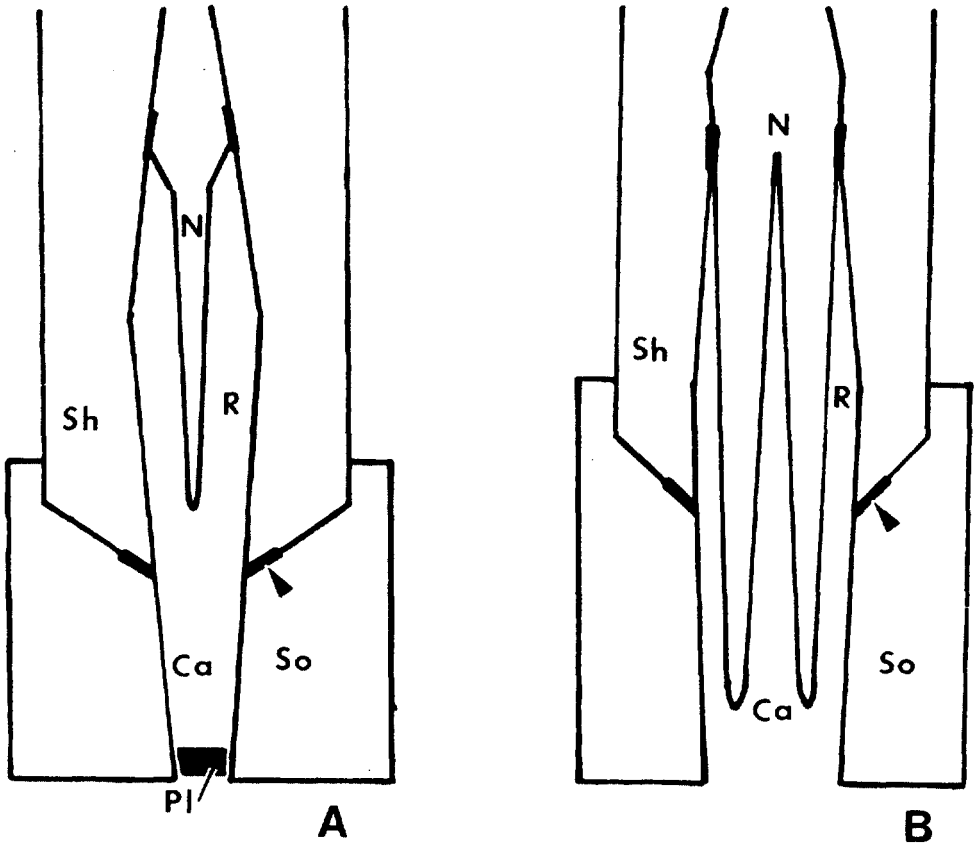

FIG. 1. Schematic diagram of phasmids. A) *Heterodera schachtii.* B) *Caenorhabditis elegans.* N = neuron, Pl = ampullar plug, R = receptor cavity, Sh = sheath cell, So = socket cell, arrows = intercellular junctions.

may terminate at the base of the receptor cavity or extend into the canal. Phasmid neuron synapses were observed in *Caenorhabditis elegans* Maupas, 1899 (48).

The phasmid is believed to be a chemoreceptor in contact with the external environment, despite the electron-dense plug reported in most species. Although developmentally related to the amphid (20, 21), its specific functions are still uncertain. Because of this functional uncertainty, selection pressures for possible convergent evolution and phylogenetic reversals of its features are difficult to evaluate in alternative phylogenetic trees. The relative degree of development of the phasmid is assessed here in different stages to provide possible functional insights.

In this study, the ampulla shape is also examined in greater detail through the developmental stages in *M. charis* to confirm its lens-like form and to test its homology or nonhomology with pore-like phasmid character states. One currently debated test of homology employs the rule that more specialized characters occur late in development. Therefore adults, including males, tend to have the most derived and therefore useful characters in a phylogenetic analysis (2). Detailed morphology of this phasmid may provide a basis for comparing the phasmids in *Heterodera, Verutus,* and other genera where they appear to be partially or completely lost (8,35).

MATERIALS AND METHODS

Meloidodera floridensis, the type species, was chosen as a model for other species in the genus because males will develop in water without a host plant (21,45). *Meloi-*

dodera floridensis was cultured in the greenhouse on slash pine, *Pinus elliotii*. Feeder roots were placed in a mist chamber and second-stage juveniles (J2) were collected every 2 to 3 days over a period of 3 weeks. These J2 were kept in tap water in Stender dishes for 2 months at 21.5–24.5 C and transferred weekly to clean water. During this time a high proportion of the population developed into immature third-stage males (M3), immature fourth-stage males (M4), and mature adult males (M5) as a direct result of starvation-induced male sex determination. Intermediate M3 and M4 stages could be discerned by counting cuticles (21,45) and selecting individuals with the most distinct stylets. These stages were also selected from soil sievings. Individuals still in the molt phase were identified with the TEM for assessing the sequence of molting events by changes in body wall morphology (4,43).

Meloidodera charis was collected from wild peonies, *Peonia californica,* in Badger Canyon, San Bernardino, California. Feeder root pieces were placed under mist for 5 days; males were selected and fixed 2 days later. An Arizona population was grown on pinto bean, *Phaseolus vulgaris* (17), and J2 and early M5 stages were dissected from the roots. The M5 was identified by the presence of rudimentary spicules. First-stage juveniles (J1) and early J2 stages of the Arizona population were released from the egg with a needle and identified by stylet morphology and degree of intestinal development. The J1 within the egg had obscure stylets and when released from the egg, the J1 body did not completely straighten. Unfixed specimens, unlike fixed specimens, swelled noticeably after about 1 hour.

Phasmids of at least three specimens from each stage were examined. Seven individuals of various stages were observed during the molt. Ten specimens each of J2 and M5 males were used to characterize and reconstruct phasmids by photographing cross sections and longitudinal sections at intervals of 2–6 sections. Two methods of fixation were employed; one had been used for a phasmid study of *Heterodera schachtii* Schmidt, 1871 juveniles (1), and the other was a modification of a method used for *C. elegans* (6). This modification included use of embedding capsule baskets with 25-μm nylon mesh for transfers (12), 0.2 M cacodylate buffer at 60 rather than 70 C, and puncture of the body after 1 hour of fixation with an eyeknife or electrochemically sharpened tungsten needle (22).

Specimens were embedded in 2% water agar, which was cut into blocks for proper orientation, dehydrated in an acetone series, and infiltrated with Spurr's epoxy. Serial sections were cut with a Sorvall 6000 ultramicrotome. Silver sections were placed on formvar-coated 200-mesh hexagonal grids stained with uranyl acetate for 30 minutes and Reynolds lead citrate for 5 minutes. Specimens were viewed with a Hitachi H-600 transmission electron microscope at 75 kV.

Voucher specimens of J2 and M5 are deposited in the University of California, Riverside Nematode Collection (UCRNC).

Results

Second-stage juvenile and adult male phasmids: The phasmid is similar in form but becomes smaller from the J2 to the M5 male of both *M. floridensis* and *M. charis* (Figs. 2, 3). Height of a typical M5 phasmid from the ampulla to the top of the neuron nucleus and diameter at the level of the receptor cavity are about 60% of those of the J2.

The sheath cell of the phasmid is bounded on the lateral side by the hypodermal seam cell; this boundary is indicated by small intercellular junctions (Fig. 4A′). On either side of the seam cell are two socket cells that wrap half way around the sheath cell and meet near the middle of the intestinal side of the sheath cell (Fig. 4A). Nuclei of these socket cells may lie on the inner side of the sheath cell (Fig. 4A) or to one side of the sheath and seam cells when extensive lipid occurs in the intestine.

Canals of the phasmids on each side of the body meet their sheath cell receptor cavities on the subdorsal side of the body

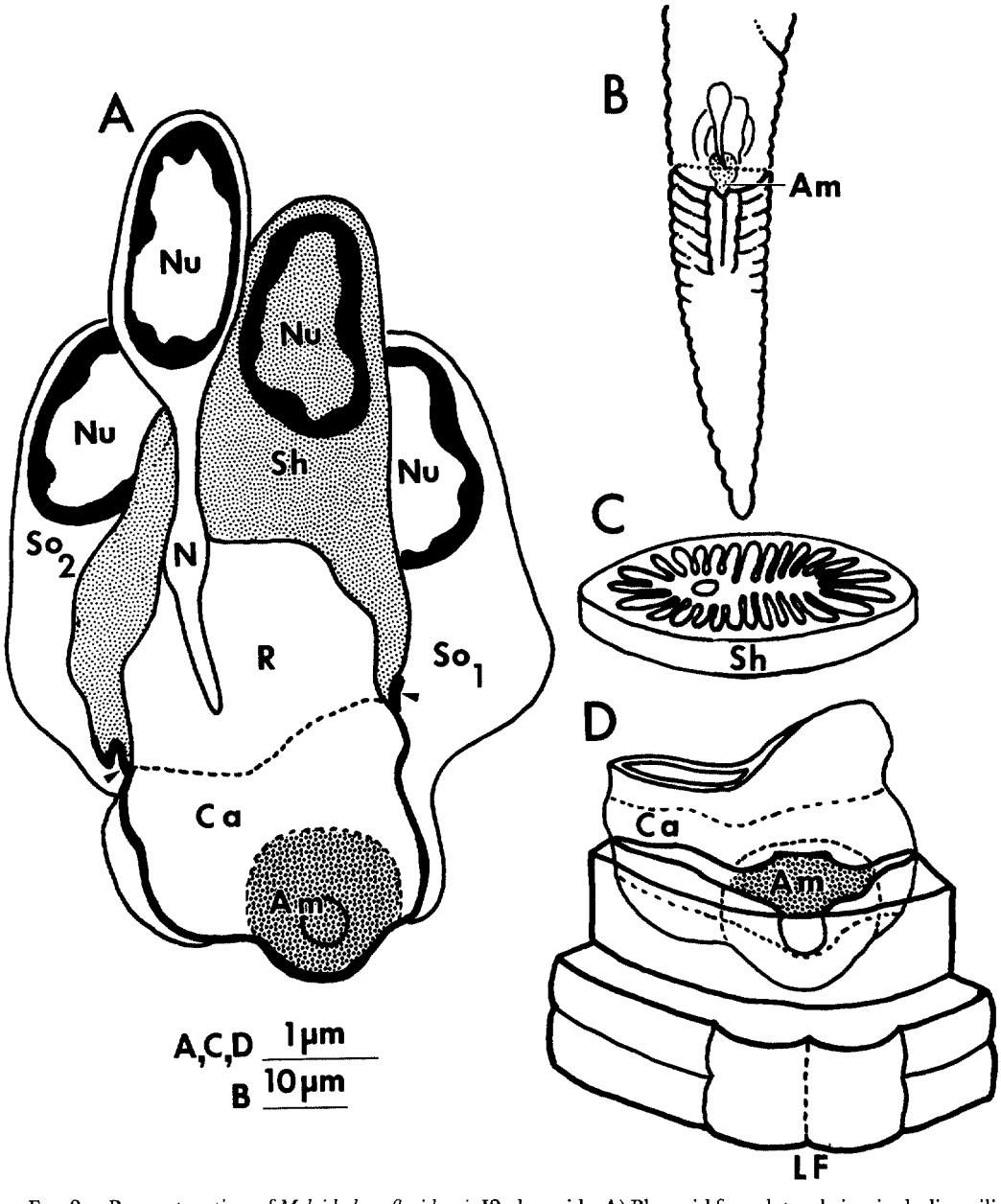

FIG. 2. Reconstruction of *Meloidodera floridensis* J2 phasmids. A) Phasmid from lateral view including ciliary neuron (N) with microtubular zones. Am = ampulla, Ca = canal, Nu = nucleus, R = receptor cavity, Sh = sheath cell, So_1 = socket cell 1, So_2 = socket cell 2, arrows = intercellular junctions. B) Size and position of lens-shaped ampulla (Am) relative to lateral view of entire tail. Partial cross section at level of ampulla. C) Cross section of sheath cell (Sh). D) Three dimensional view from lateral field (LF) of canal (Ca) and the lens-shaped ampulla (Am) including cross section through ampulla.

(Fig. 5E). The sheath cell is surrounded by two socket cells for much of its length. Intercellular junctions delineate the base of the sheath cell and socket cells (Figs. 2, 3, 10B). Intercellular junctions surrounded by the sheath cell cytoplasm also enclose the enlarged dendrite base (Figs. 2, 3, 7D, 10B). The neuron nucleus lies just anterior and lateral to the sheath cell nucleus. In the M5, the sheath cell nucleus lies be-

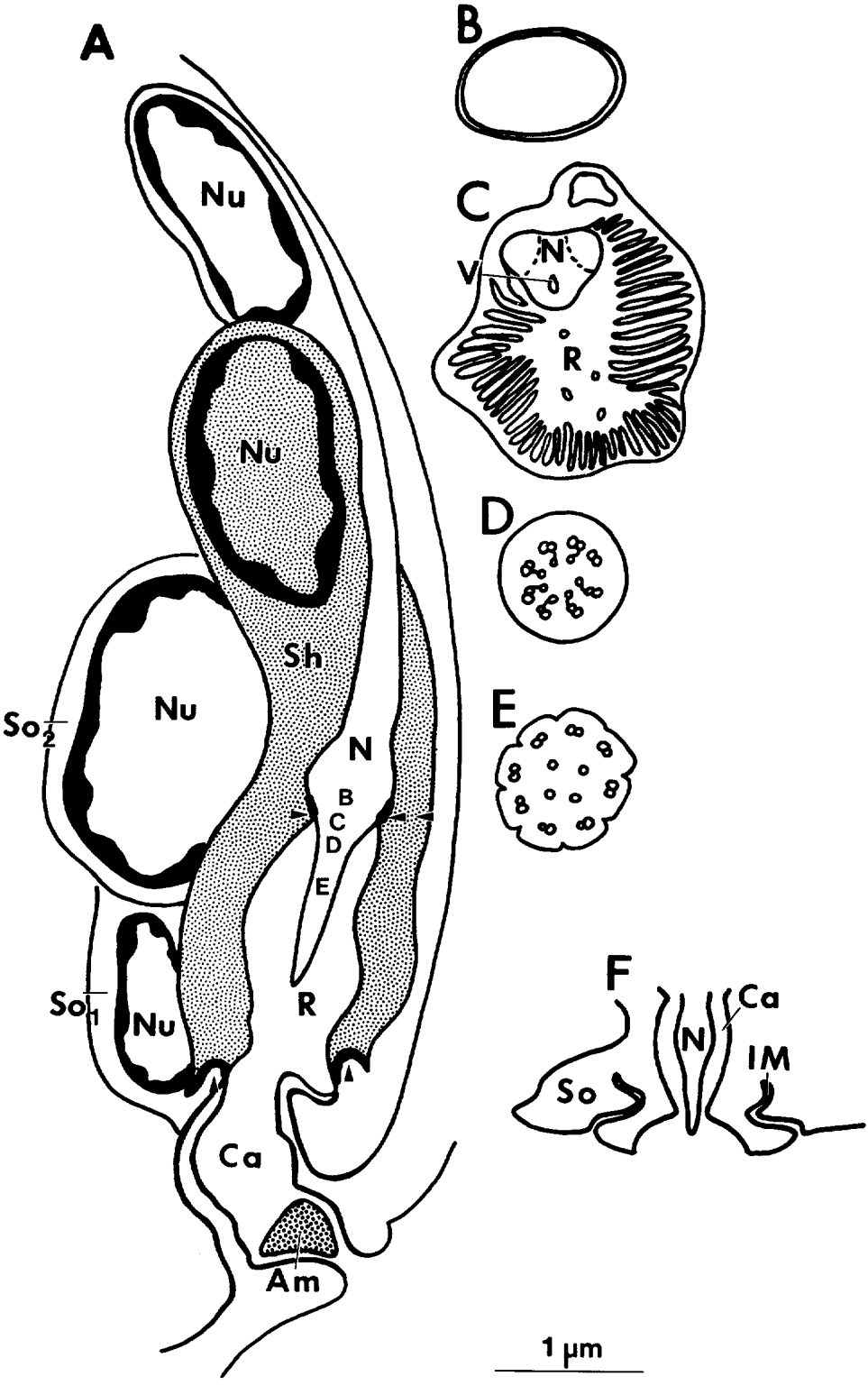
A
B
C
N
V
R
D
E
F
Nu
Nu
Nu
Nu
Sh
So_2
So_1
N
B
C
D
E
R
Ca
Am
So
N
Ca
IM
1 µm

tween the body wall muscles and the spicule retractor and protractor muscles.

Characteristics of the phasmid and body wall during molting: During the early, early-middle, late-middle, and late molting periods, a general pattern of development of parts of the phasmid is evident within the various stages. Early molt is characterized by degradation of phasmid features and muscles, early-middle molt by cuticular separation from the enlarged interchordal hypodermis, late-middle molt by hypodermal vesiculation and the beginning of cuticle layering and old cuticle resorption, and late molt by hypodermal shrinkage and cuticular maturation.

During the very early molt after root penetration, smooth endoplasmic reticulum (SER) in *M. charis* J2 becomes prominent in the hypodermis and in the degenerating sheath cell (Fig. 5D). The receptor cavity secretion is present, but sheath cell lamellae are degenerated. A small portion of the dendrite apparently buds into the receptor cavity. There is no evidence of a canal or ampulla.

During cellular enlargement of the early-middle molt, the cuticle is completely separated from the hypodermis and the outer layer of the new external cortex appears on the outer edge of the hypodermis. There is no evidence of a secreted electron-dense plug. A dense inclusion body is characteristically present adjacent to the socket cell nucleus (Fig. 6B). A distal segment of the dendrite, which may show singlet microtubules (Fig. 6A′, C, D), exists during the molt but is absent in stages after molts. At this time the exceptionally large hypodermal cells contain extensive rough endoplasmic reticulum and some Golgi complexes (Fig. 6B). The basal lamina associated with muscle fields outlines the apparent pseudocoelom which is most evident at this time in development (Fig. 6A). The basal lamina is adjacent to the inner lateral side of the narrow sheath cell.

In the late-middle molt, the old cuticle begins to dissolve, and differentiation of layers begins in the new cuticle. The neuron and canal may be turned 90 degrees from their usual position (Fig. 7A). The neuron at this time has rootlets in the enlarged dendrite base, and the distal segment of the dendrite is irregularly shaped and contains vesicles.

During the late molt, newly differentiated cuticle undergoes maturation of its layers. A *M. charis* J1 within the egg during the late molt can be used to describe phasmid secretion characteristics. These secretions are also visible in slightly later molt J2 individuals of both species.

In late embryo-early J1, all of the surfaces of the socket and sheath cells are bounded by intercellular (probably tight) junctions. The receptor cavity and neuron of the J1 are completely formed. The lining of the wide canal and ampulla, however, is not completely deposited (Fig. 5A). A dark secretion occurs from the receptor cavity to the canal, ampulla, and around the external cuticle. A secretion of similar texture and density is continuous from the rectum to the body wall cuticle as well. This secretion also occurs in prehatch J2 of both species. The more mature premolt cuticle of these J2 was an indication that the secretion probably had dissipated from the outer cuticle.

Ampulla: All fully developed stages have an ampullar opening with a cuticular lining containing a dark plug. This internal cuticular lining is continuous with the outer cuticle. During certain periods of molting, there is no ampullar opening or plug. For

←

FIG. 3. Reconstruction of *Meloidodera floridensis* M5 phasmid. A) Phasmid from dorso-ventral view. Am = ampulla, Ca = canal, N = neuron, Nu = nucleus, R = receptor cavity, Sh = sheath cell, So_1 = socket cell 1, So_2 = socket cell 2, arrows = intercellular junctions. B–E correspond to cross sections as follows: B) Neuronal region above neuron-sheath junction. C) Lamellar-anastomosis dendrite zone of neuron (N) with vesicles (V) and receptor cavity (R). D) Transition zone of neuron. E) Middle segment of neuron. F) Longitudinal view of infolded membranes (IM) of socket cell (So) surrounding neuron at the molt. Ca = canal, N = neuron.

example, the early molt postpenetration *M. charis* J2 loses the old ampulla and canal, and only the old neuron with its poorly formed receptor cavity remains (Fig. 5D). In *M. floridensis* and probably in *M. charis*, middle molt M3, M4, and M5 have new canals and neurons, but no openings to the exterior. Late molt J1 and J2 of both species have rudimentary ampullar openings where the cuticle is being deposited and the electron-dense plug is accumulating (Fig. 8D) to form the ampulla of the next juvenile stage (Fig. 8E). Instead of the socket cell directly depositing the ampullar cuticle, vesicles from the active hypodermis (Fig. 8D) and possibly some plug secretion (Fig. 8E) appear to form the ampullar cuticle. The final plug often contains a dark, crystalline differentiation on its outer surface (Fig. 8E).

Ampullae of post-hatch *M. floridensis* J2 in cross section have the shape of a large lens (Figs. 2, 8E, 9B). The incompletely formed ampullae of prehatch *M. charis* J2 are approximately the size and shape of the large posthatch lens of *M. floridensis* J2 (Fig. 9B). Ampullae in the M5 of both species are smaller than in the J2. The lens shape becomes somewhat elongated, forming a more rhomboid opening (Fig. 9B).

Canal and socket cells: The posterior ends of all socket cells form intercellular junctions with the adjacent hypodermal and sheath cells. The canal of J2 of both species is large and crescent shaped in cross section (Fig. 5E). The M3 has an unusually short canal, relative to the J2, and the M5 has the longest, narrowest canal (Figs. 2, 3). Late molt canals are wider than the canals after the molt.

In prehatch *M. floridensis* J2, both socket cells are filled with double intracellular membranes. The socket cells are larger than in the posthatch J2. Near the junctional complexes defining the canal within the socket cell, secretions associated with intracellular double membranes accumulate around the periphery of the canal. These electron-dense secretions are closely associated with the developing cuticle during this late phase of the molt (Fig. 8A). In fully developed stages, dark material sim-

→

FIG. 4. *Meloidodera floridensis* J2 phasmid cross sections. A) Posthatch J2 with two socket cell nuclei (SoN_1 and SoN_2). From lateral view, socket cell 1 is adjacent to right side of hypodermal seam cell (Sc). Socket cell 1 encircles ampulla and lower canal in counterclockwise direction. Socket cell 2 surrounds upper canal and sheath cell in clockwise direction. G = glycogen, L = lipid, arrows = intercellular junctions. Inset A') Intercellular junctions of seam cell (arrows). B) Multivesicular body (MVB) and multilamellar body (MLB), adjacent to socket cell nucleus (SoN).

FIG. 5. *Meloidodera charis* and *M. floridensis* canal and receptor cavity cross sections. A) *M. charis* J1 with incompletely formed ampulla (Am). Dots indicate boundary between sheath cell (Sh) and receptor cavity (RC). Ca = canal, Cu = outer cuticle, SE = secretion, So = socket cell, SC = Seam cell. B) Prehatch J2 at base of sheath cell receptor cavity (R). DN = distal neuron, EA = end apparatus of canal, L = lamellae, P = pocket. C) Prehatch J2. Oval neuron region (N) with vesicles (V) near junction with sheath cell, L = lamellae, P = pocket, R = receptor cavity. D) Postpenetration J2. Neuron (N) with bud (arrow) in receptor cavity (R) of degenerating sheath cell (Sh). SER = smooth endoplasmic reticulum. E) *M. floridensis* J2, crescent-shaped canal (Ca) extending from socket cell on right (So) to sheath cell (Sh) on left. Do = dorsal side.

FIG. 6. *Meloidodera floridensis* middle molt, phasmid cross sections. A) M2 molt. Interior storage region (In) containing lipid bounded by basal lamina (arrow) continuous with left subventral muscle field (LSVM). H = interchordal hypodermis, N = neuron, SC = seam cell, Sh = sheath cell, So = socket cell. Inset A') Ciliary distal zone of neuron (N). B) M3 molt. Sheath cell (Sh) with receptor cavity (R) and neuron (N) surrounded by socket cell (So) containing dense body (DB). Hypodermal seam cell (SC) containing circular Golgi complex (G). RER = rough endoplasmic reticulum. C) M2 molt. Socket cell (So) infolded on itself with intercellular junctions (arrow) forming a star-shape. Star-shaped junctions surround electron-dense double membrane of canal (Ca). Distal ciliary neuron region (N) and vesicles (V) within the canal. D) M3 molt. Socket cell (So) encircles distal neuron (N). Intercellular junctions (arrow) of infolded membranes of socket cell surround canal membrane (Ca). M = microtubules.

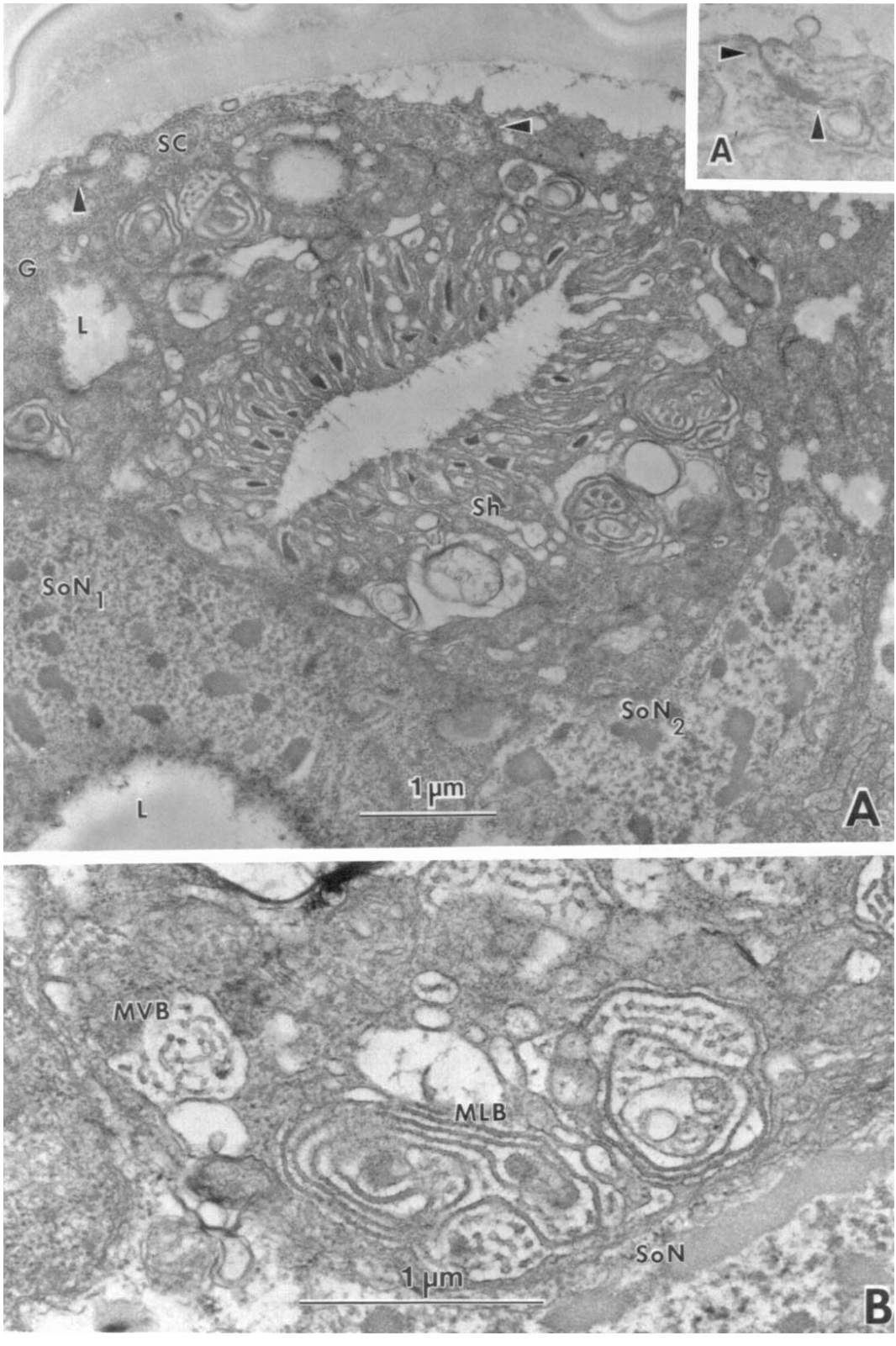
SC
G
L
Sh
SoN1
SoN2
L
1 µm
A
A
MVB
MLB
SoN
1 µm
B

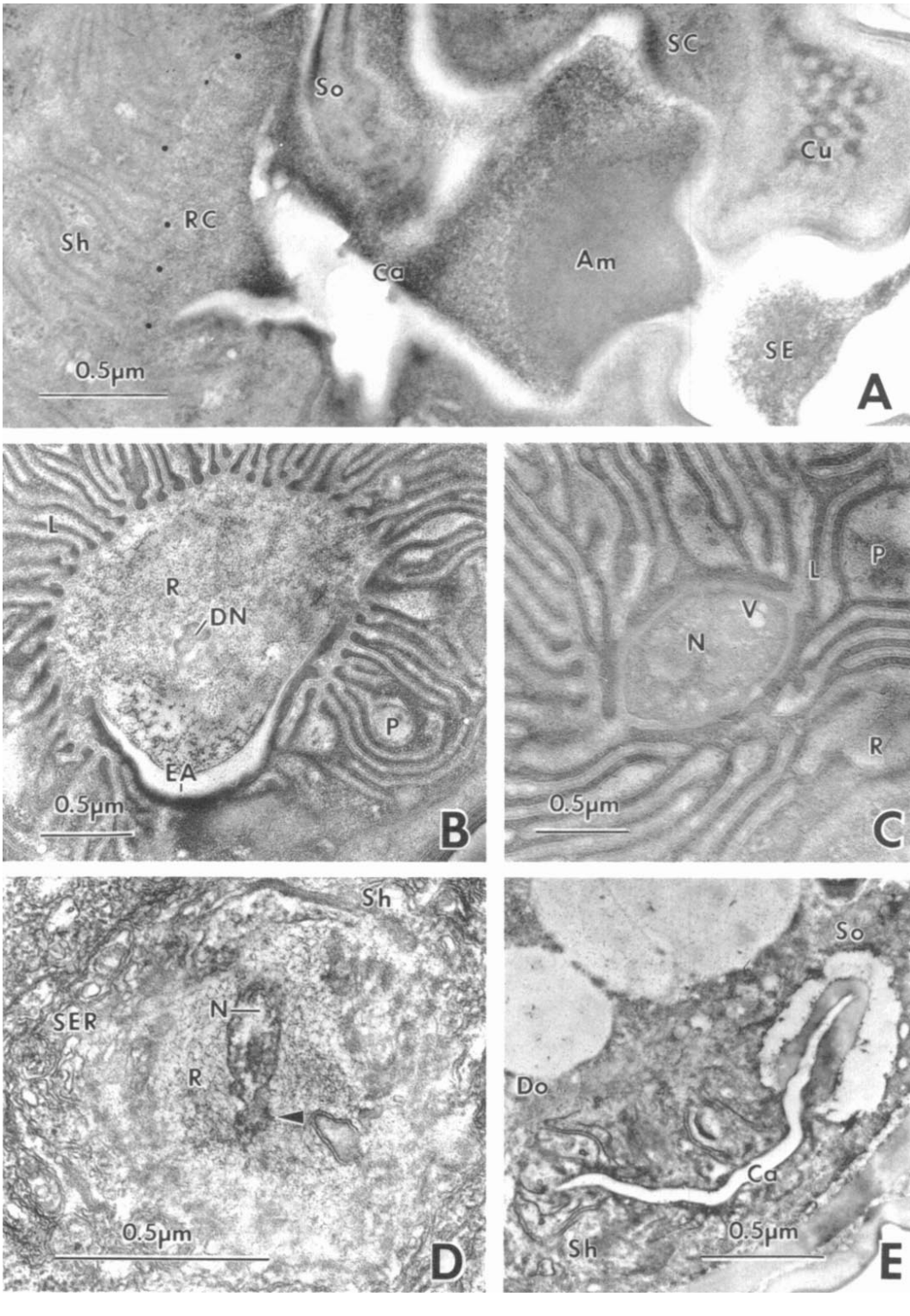
SC
So
Cu
RC
Sh
Am
Ca
SE
0.5µm
A
L
R
DN
P
EA
0.5µm
B
L
P
V
N
R
0.5µm
C
Sh
SER
N
R
0.5µm
D
So
Do
Ca
Sh
0.5µm
E

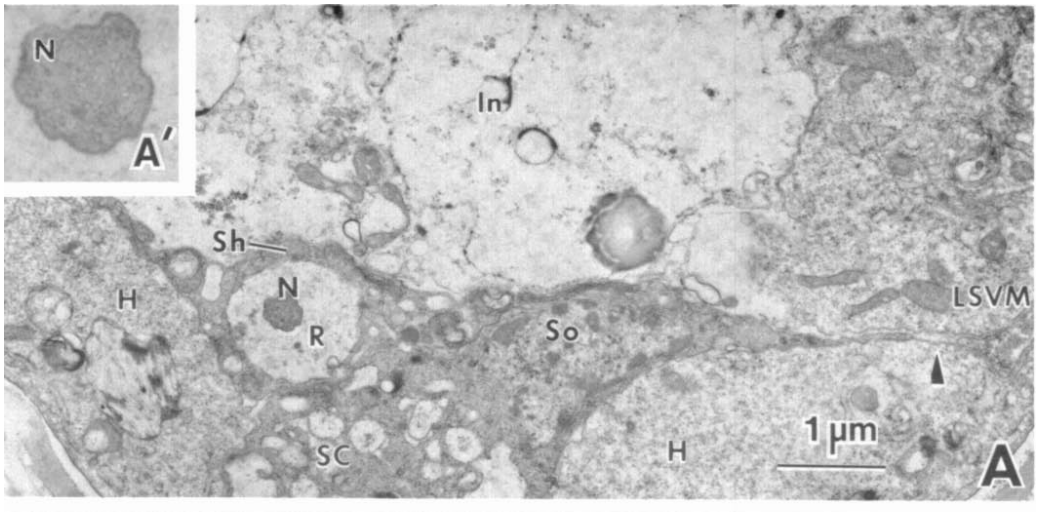
N
A′
In
Sh
H
N
R
So
LSVM
SC
H
1 µm
A

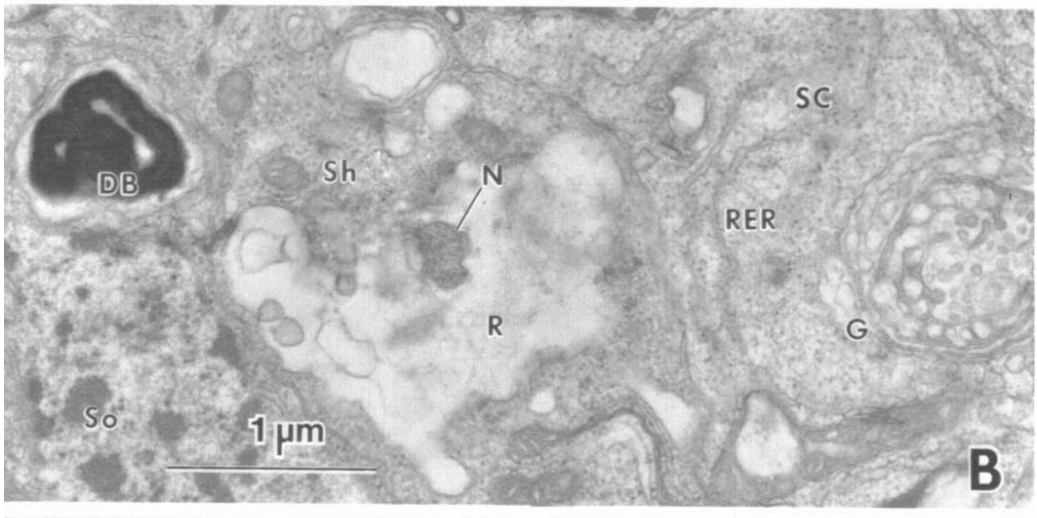
DB
Sh
N
SC
RER
R
G
So
1 µm
B

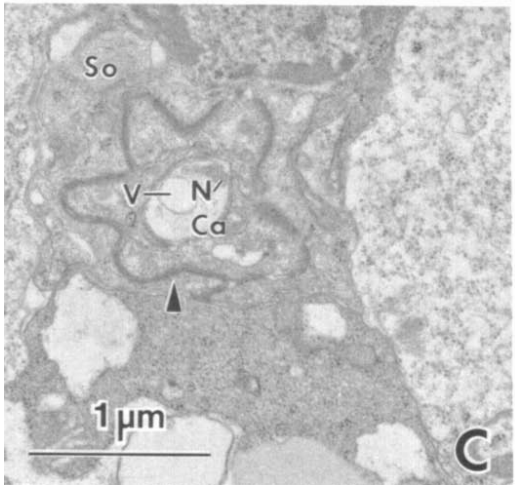
So
V
N
Ca
1 µm
C

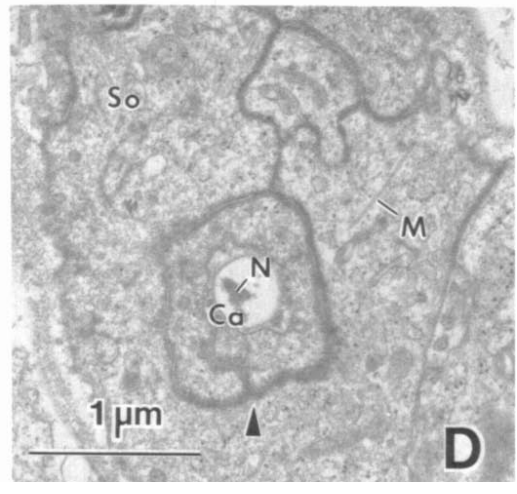
So
M
N
Ca
1 µm
D

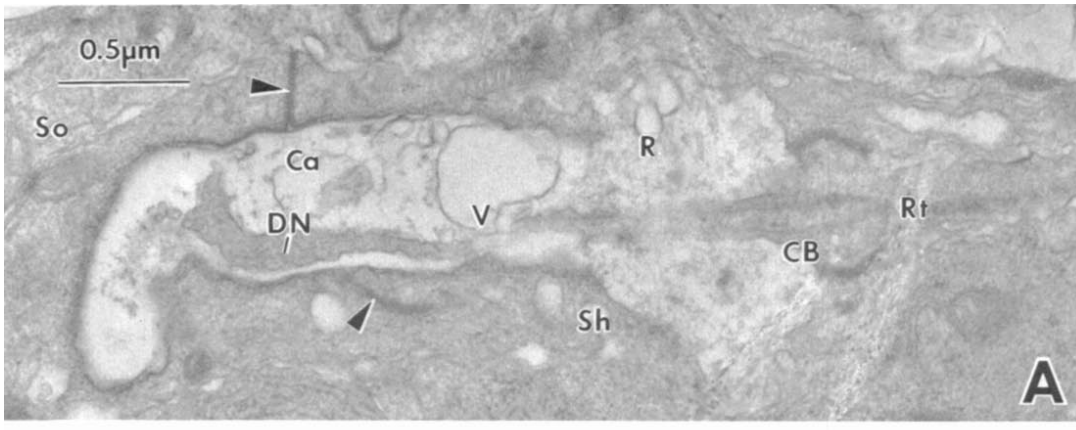
0.5µm
So
Ca
DN
V
R
Rt
CB
Sh
A

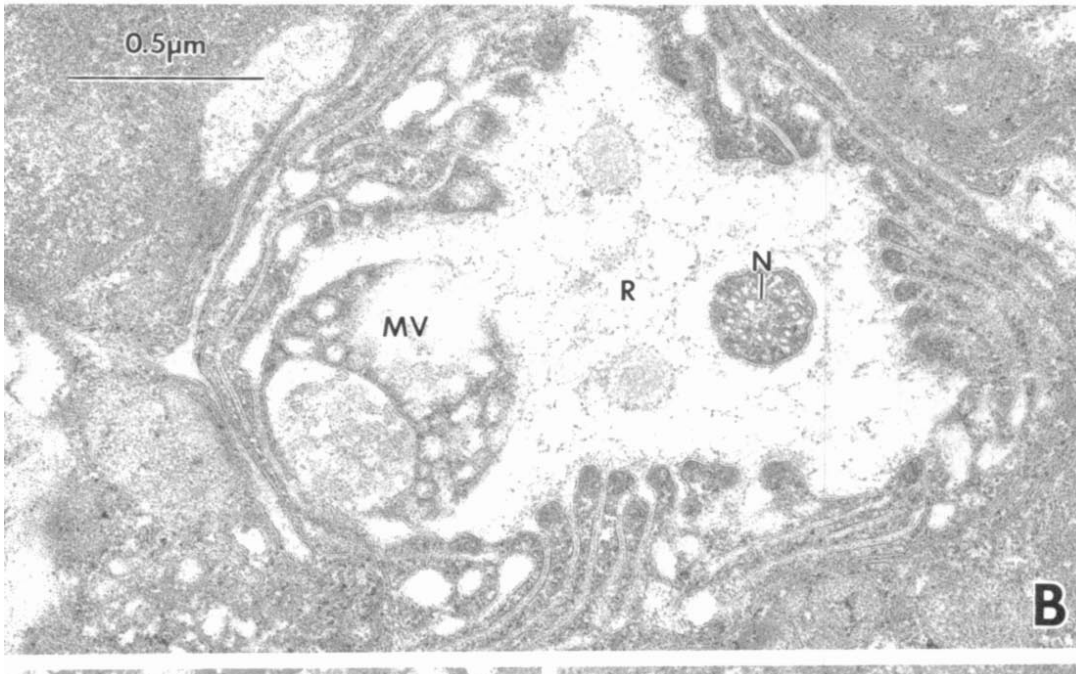
0.5µm
MV
R
N
B

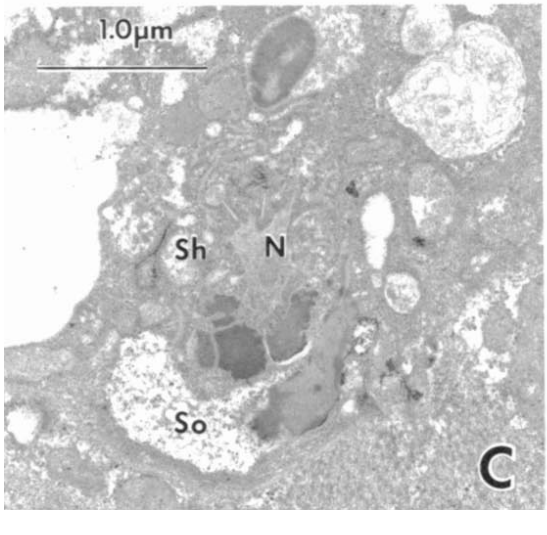
1.0µm
Sh
N
So
C

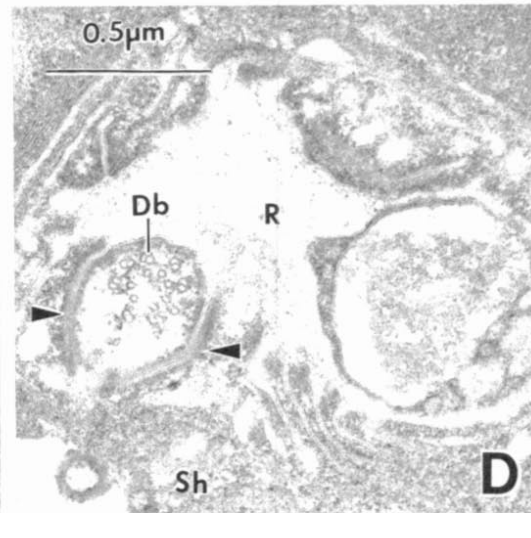
0.5µm
Db
R
Sh
D

ilar to the secretion during the molt also lines the cellular side of the canal cuticle and ampulla.

In the J2 just after hatch, the cytoplasm of the socket cells appears to contain primarily glycogen and lipid (Fig. 4A). After molts, the socket cells degenerate in all stages. A typical example is an aged M5 specimen with a socket cell largely defined by the remnants of the surrounding intercellular junctions and with little cellular material around the distal base of the canal (Fig. 7C). Often a dark deposit, similar to the substance of the ampulla plugs, is found at the base of this aging cell.

During middle molts, before any cuticle or ampullar opening exists in any stage, a rudimentary canal defined by a double membrane is visible (Figs. 3F, 6C, D). This double membrane is situated surprisingly close to the phasmid opening. The socket cell folds in on itself in the longitudinal plane (Fig. 6C, D). Horizontally the socket cell forms a doughnut shape around the canal with a seam readily identified by an intracellular junction. Microtubules are visible on close inspection in the outer region of the socket cell (Fig. 6D). The canal contains the distal segment of the neuron for most of its length (Figs. 6C, D; 7A).

A cuticular extension of the canal exists at the beginning of the sheath cell receptor cavity. This canal extension or end apparatus (Fig. 5B) appears to merge with a sheath cell lamella before the cuticle is completely laid down in prehatch individuals.

Neuron: Dendritic ciliary regions in these phasmids contain eight microtubular doublets and 2–6 central singlets. This pattern occurs between the middle segment and the transition zone of the dendrite (Fig. 3D, E). Doublets of the transition zone of the cilium contain 13 + 11 fibrils. A ciliary segment close to the region where a basal body would be expected to occur contains eight doublets with tenuous connections to seven singlets (Fig. 7D). The middle segment membrane of the cilium has eight lobes (Fig. 3E). As the neuron approaches its junctional connection with the sheath cell, it becomes triangular to oval with central and lateral vesicles (Figs. 3C, 5C). Above the tight junctions in the distal dendrite base, vacuoles are usually found in intermolt dendrites (Fig. 10). At middle molt, the distal dendrite base contains rootlets (Fig. 7A).

During all observed molts, an extended dendrite is seen within the canal (Figs. 6C, D; 7A). The shape of this distal zone is irregular, appearing to be in the process of vesiculation (Figs. 6C, 7A). Above this irregular region, the dendrite region in the lower receptor cavity contains single microtubules (Fig. 6A'). These distal regions are absent in postmolt neurons. Then the dendrite terminates at the beginning of the receptor cavity, just inside the end apparatus of the canal (Fig. 5B). In one male, determined to be a young M5 on the basis of spicule maturity, the middle ciliary segment of the dendrite still extended slightly into the end apparatus of the canal. (Fig. 12).

Receptor cavity and sheath cell: Phasmids of prehatch J2 of *M. floridensis* are extremely large in cross section (Fig. 8B, C). The cross sections of sheath cells at the level of the receptor cavities comprise an unusually large (nearly 75%) area of the tail. Sheath cells have enormous numbers

←

FIG. 7. *Meloidodera floridensis* and *M. charis* cross sections of phasmid. A) *M. floridensis*, M4 molt. Dendrite shifted 90 degrees from intermolt position, resulting in longitudinal orientation. Rootlet region (Rt) above ciliary base (CB). Distal ciliary region (DN) with neurotubules and vesicles. Intercellular junctions (arrow) separate sheath cell (Sh) from socket cell (So). Ca = canal, R = receptor cavity, V = vesicle. B) *M. charis* M5. Neuron (N) and receptor cavity (R) with multivesicle (MV). C) *M. charis* M5. Phasmid with neuron (N) and degenerate socket cells (So) and sheath cells (Sh) containing dense deposits. D) *M. charis* M5. Receptor cavity (R) with neuron and intercellular junctions (arrows). Neuron is near level of transition zone close to basal body and includes eight microtubule doublets (Db) and eight singlets.

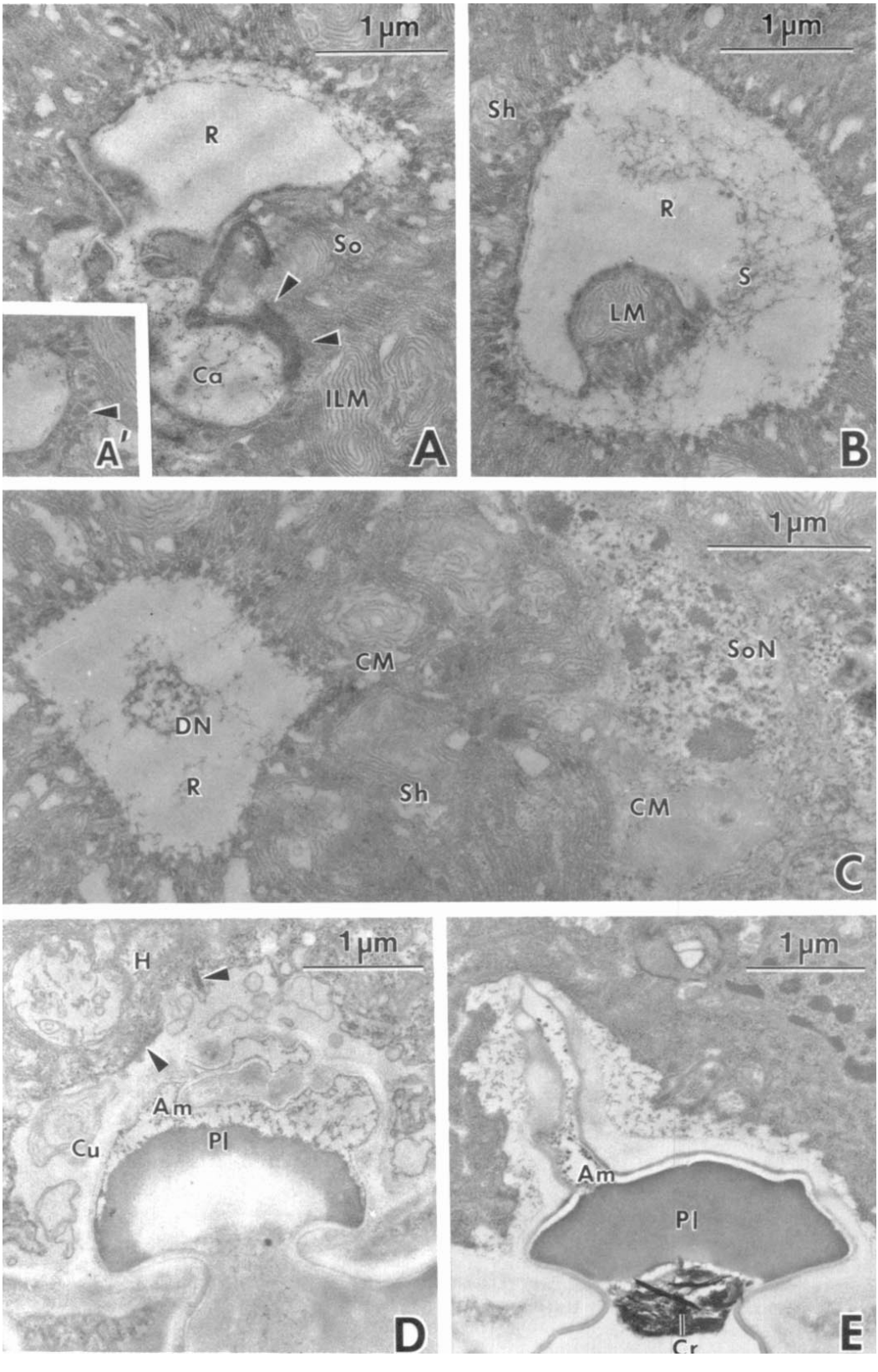
1 µm
R
So
Ca
ILM
A'
A
1 µm
Sh
R
S
LM
B
1 µm
CM
SoN
DN
R
Sh
CM
C
1 µm
H
Am
Cu
Pl
D
1 µm
Am
Pl
Cr
E

of closely apposed lamellar membranes associated with a secretion that is especially dense at the inflated inner tips (Fig. 8A–C). These tips surround a large receptor cavity that is circular below the level of the neuron (Fig. 8B). Near the level of the transition zone of the neuron, the receptor cavity is broadly fusiform (Fig. 8C).

Membranes are in various forms of differentiation. At some points in development double membranes are essentially perpendicular to the long axis of the cell, whereas at other points of development they are nearly parallel or circular. Some double membranes have distinct extracellular space between them, whereas others do not. Concentric membranes identical to those on the periphery of the sheath cell exist in a thin row of socket cell nuclei separating the two sheath cells (Fig. 8C). Concentric membranes are regularly spaced between the more-or-less perpendicular lamellae extending to the periphery of the cell. These concentric membranes are occasionally expelled into the receptor cavity (Fig. 8B). The average size of a membrane infolding is 0.03 μm wide × 0.15 μm long in *M. floridensis*; in prehatch *M. charis* the infoldings surrounding the circular receptor cavity are slightly thicker (0.04 × 0.13 μm) (Fig. 5B, C). Some infoldings anastomose with others at various points including the tips (Fig. 5B). Anastomosing lamellae may lie adjacent to the neuron (Fig. 5C) or adjacent to the internal terminus of the canal at the receptor cavity (Fig. 5B). This canal region is also called the end apparatus.

Characteristic oval, inflated pockets may contain secretions (Fig. 5B, C). These pockets sometimes contain concentric membranes or vesicles. The membrane secretion extends from the receptor cavity through the wide canal and accumulates most densely at the outer rim of the large ampulla. Anastomosed lamellae lie adjacent to the end apparatus where the secretion is more condensed than in the receptor cavity (Fig. 5B).

In the posthatch J2 in cross section, the

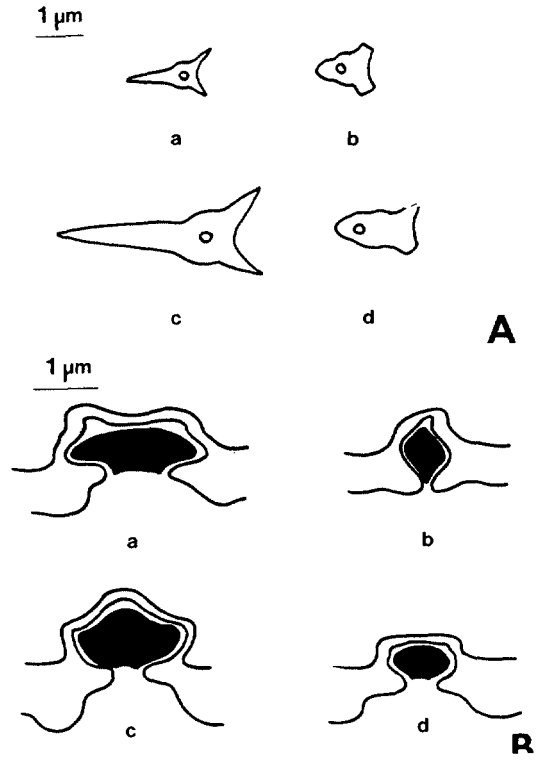

FIG. 9. Comparison of reconstructed receptor cavities and ampullae of *Meloidodera floridensis* and *M. charis*. A) Receptor cavity (cross section) of *M. charis* J2 (a) and M5 (b) and *M. floridensis* J2 (c) and M5 (d). Cellular details shown in Figures 2C and 5. B) Large lens ampulla (longitudinal section) of *M. floridensis* J2 (a) in relation to elongated rhomboid ampulla in M5 (b). Small lens ampulla of *M. charis* J2. It is enlarged in the prehatched J2 (c) and becomes reduced after hatch (d).

←

FIG. 8. *Meloidodera floridensis* J2 phasmid cross sections. A) Prehatch J2 canal (Ca) surrounded by dense secretion (arrows) from intracellular lamellar membranes (ILM) in socket cell (So). R = Receptor cavity. Inset A') Secretion concentrated at periphery of canal. B) Lamellar membranes (LM) and secretions (S) from sheath cell (Sh) in receptor cavity (R). C) Prehatch J2 receptor cavity (R). CM = concentric membranes, DN = distal neuron, SoN = socket cell nucleus, Sh = sheath cell. D) Prehatch J2 plug material (Pl) filling ampullar (Am) region. Cuticular matrix (Cu) is deposited by hypodermis (H). E) Posthatch J2 ampulla (Am) with amorphous plug (Pl) and dark outer crystals (Cr).

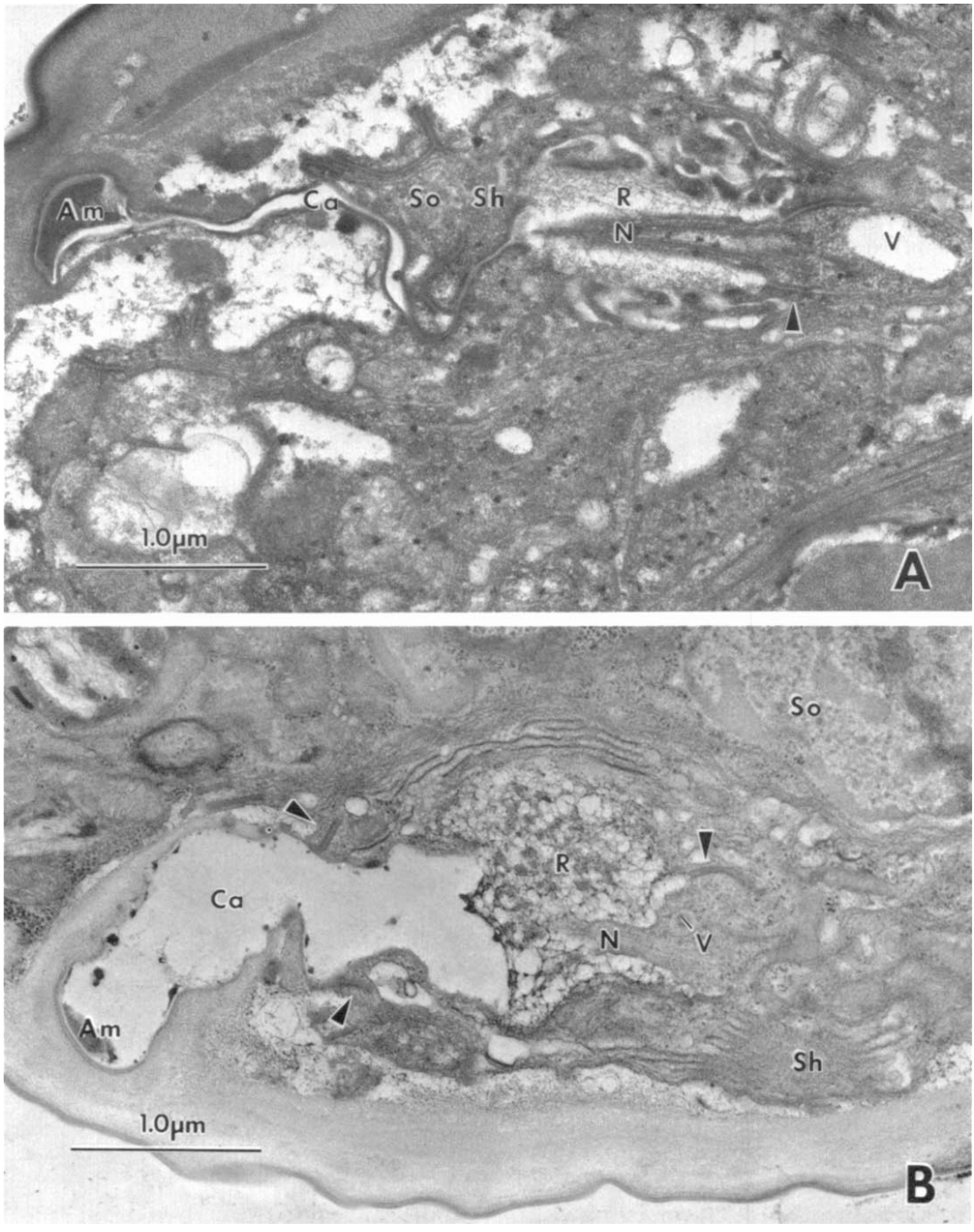

FIG. 10. Longitudinal sections of M5 phasmids. A) *Meloidodera charis*. B) *Meloidodera floridensis*. Am = ampulla, Ca = canal, N = neuron, R = receptor cavity, Sh = sheath cell, So = socket cell, V = vacuole, arrows = intercellular junctions.

receptor cavity at certain levels may appear slit-like or fusiform, but the cavity is essentially Y shaped at the level of the ciliary transition zone (Fig. 11). The Y has a slight inflation at the branch point. *Meloidodera charis* has a shorter Y-shaped cavity than *M. floridensis* (Fig. 9A).

Freshly extracted *M. floridensis* J2 show some variation in form of sheath cell membranes. Membranes of the lamellae are

continuous with the plasma membrane and inflate to varying degrees (Fig. 11). The vesicles of the sheath cell are very small when double membranes are so closely apposed that lamellae are not formed between them (Fig. 11B, C). Another form of sheath cell has highly inflated interlamellar spaces (Figs. 8D, E; 11A) and contains relatively large multivesicles, multilamellae, lamellar anastomoses, and dense cytoplasm.

From the previous descriptions, an inferred sequence of events can be summarized for both species. Before hatching, membranes of lamellae are numerous and may be either closed or inflated near the receptor cavity. Inflation is greatest just before and after hatch. After hatch, the receptor cavity flattens in on itself and peripheral membranes undergo vesiculation and lysis. Lamellae anastomose at their tips, forming a smooth boundary to the receptor cavity. Inside the cell, reclosed membranes form successive internal vacuoles. By the beginning of the molt, the inner membranes have been transformed or disintegrated.

Four specimens were observed in the ephemeral fourth stage. Only toward the end of the molt, before the cuticle had differentiated, was the phasmid visible with the neuron extending into the canal. In the other specimens where the cuticle was differentiated, no phasmid was apparent.

The early fifth-stage male has a sheath cell with especially long lamellae (Fig. 12). Some of these lamellae radiate around the large end apparatus which encloses the beginning of the neuron at the junction of the canal and receptor cavity. Most adult male phasmids have a degenerated and vacuolated sheath cell. The sheath cell and receptor cavity of the adult are smaller than those of the J2 (Fig. 9a). The lamellae are generally perpendicular to the long axis of the receptor cavity in cross section. Sometimes, however, the lamellae appear roughly parallel to the sides of the oval or Y-shaped receptor cavity (Fig. 7B). Occasionally large multivesicles are released into this cavity. Lamellae are thinner and more closely packed together in *M. floridensis* than in *M. charis* (Figs. 7B, 10A, B).

Discussion

The approximately 35 specimens observed in this study mostly included the readily accessible J2 and M5. Even within these stages, minor variability occurred in degree of natural degradation, apparently associated with age of nematode and phasmids; however, the number of specimens is sufficient to infer developmental trends and morphologically unique features. The M3 and M4 stages and molts, while represented by relatively few specimens, have been essential to understand the overall developmental sequence indicated by more comprehensive observations in J2 and M5.

Phasmids in all the stages of *Meloidodera* should be compared with other heterodderine genera, including those in which the phasmid may be partially or completely lost in adults (8,35).

Ampulla: The ampulla is the most stable feature of the phasmid in all stages. Aspects of both ampullar form as well as ampullar plug content will be carefully considered for phylogenetic value. Results of this study indicate that the cuticle-like matrix surrounding the ampulla is formed at the end of the molt from secretions of the hypodermis rather than the socket cell.

The large lens-shaped ampulla of *M. floridensis* is smaller in later developmental stages, as well as after the molt in a given stage. For instance, the smaller lens of *M. charis* is considerably larger before hatching and appears similar in size and shape to the ampulla of posthatch *M. floridensis*. Thus the ampulla of *M. floridensis* J2 may represent a developmentally earlier form of phasmid than that of *M. charis*. A similar phenomenon occurs among species of filarial nematodes regarding the degree of differentiation of cells present in the first-stage microfilaria (24).

It is important to distinguish between ampulla shape and ampulla size. Through development in these species, the opening becomes smaller, but its essential shape re-

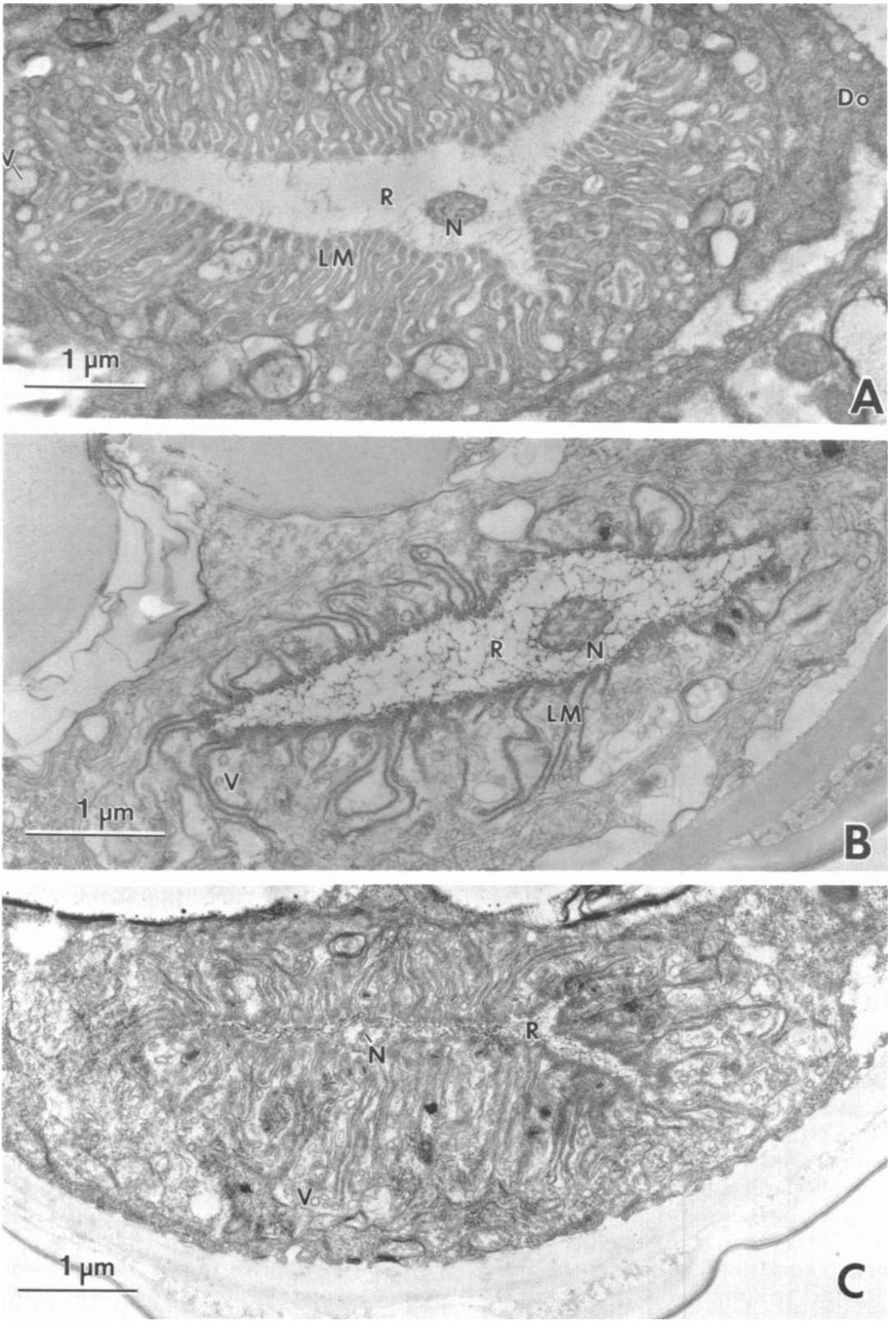
Do
V
R
N
LM
1 µm
A
R
N
LM
V
1 µm
B
R
N
V
1 µm
C

mains constant. The rhomboid ampulla of M5 is basically an elongated lens shape.

It has been noted that the size of the ampulla is correlated with the relative surface area of the membranes of sheath cell lamellae. In future studies, ampulla size may serve as a predictive index of lamellar membrane surface area in other phasmids. An understanding of the function of the lamellar surface may be helpful in future studies of the possible adaptive benefit of relatively large phasmid ampullae.

Ampullar plug content: Because of the release of lamellar membranes from the sheath cell into the receptor cavity, it is possible that lipoproteins are components of the ampullar plug and the cuticle glycocalyx. In insects, lipoprotein deposits in the pores of chemosensilla are believed to act as hydrophobic filters for lipid-soluble substances (18). Acetone aids in the penetration of water-soluble precursors of the cobalt sulfide stain for sensory organs in insects (40). It also aids in the penetration of this stain into nematode phasmids (8), presumably by solubilizing the ampullar plug.

These plugs and the plugs observed in other plant-parasitic genera (1,9,47) have a darker, sometimes crystalline differentiation on the outer surface of the ampullar opening. This dark material has the appearance of a highly condensed form of wax found on the cuticles of some juvenile insects (28,29). The filamentous liquid-crystal, lipid-water wax precursors in insects also appear similar to the filamentous substructure of the ampullar plugs in *Hoplolaimus* and *Scutellonema* (9). This structural variation in ampullar plugs could indicate the possible usefulness in chemotaxonomy, as waxes are in insects (46).

Timing of the deposition of the plug secretion on the surface of *Meloidodera* cuticle at the end of the molt and timing of wax deposition from insect glands are similar (49). Besides affecting cuticular permeability, lipids and waxes are believed to protect insects from fungal attack (29). If the phasmid, which is specific to Secernentea, definitively could be shown to secrete lipid and wax onto the cuticle, aided perhaps by the trough-like lateral incisures adjacent to the ampulla, it would be consistent with Paramonov's hypothesis that soil fungi present a selection pressure for relatively impermeable cuticles in terrestrial secernentean nematodes (36).

The secretion seen on the outer cuticle and in the ampulla of the first stage is probably a common feature at the end of all molts. This secretion may be a source of the glycocalyx on the cuticle surface, believed to be important in host and fungal parasite recognition. Glycocalyx glycosaminoglycans were proposed to be secreted from nematode sensory organs (53). Acid mucopolysaccharides (glycosaminoglycans) have been histochemically detected in the phasmid of an animal parasite (33). Glycosaminoglycans are believed to be processed in Golgi vesicles (38). There is nothing to preclude these substances from being secreted in phasmid vesicles, along with lipids and proteins in the secretion, although the relative proportions of these substances may change with time. There is a possible parallel in insects where the outermost layer of the cuticle contains a mucopolysaccharide cement mixed with wax (29).

←

FIG. 11. *Meloidodera floridensis* posthatch J2 sheath cell cross sections. A) Open membrane, open receptor cavity (R) form. Lamellar membranes (LM) entirely extracellular. Y bifurcation of cavity at dorsal (Do) end of sheath cell. Neuron (N) at level of transition zone. V = vesicles. B) Closed membrane, open receptor cavity (R) form. Lamellar membranes (LM) partially extracellular, mostly intracellular. Cavity open, just below bifurcation. Neuron (N) at level between middle segment and transition zone, slightly distal to neuron pictured in Figure 12. V = vesicles. C) Closed membrane, closed receptor cavity (R) form. Neuron (N) at transition zone level as in Figure 12. V = vesicles.

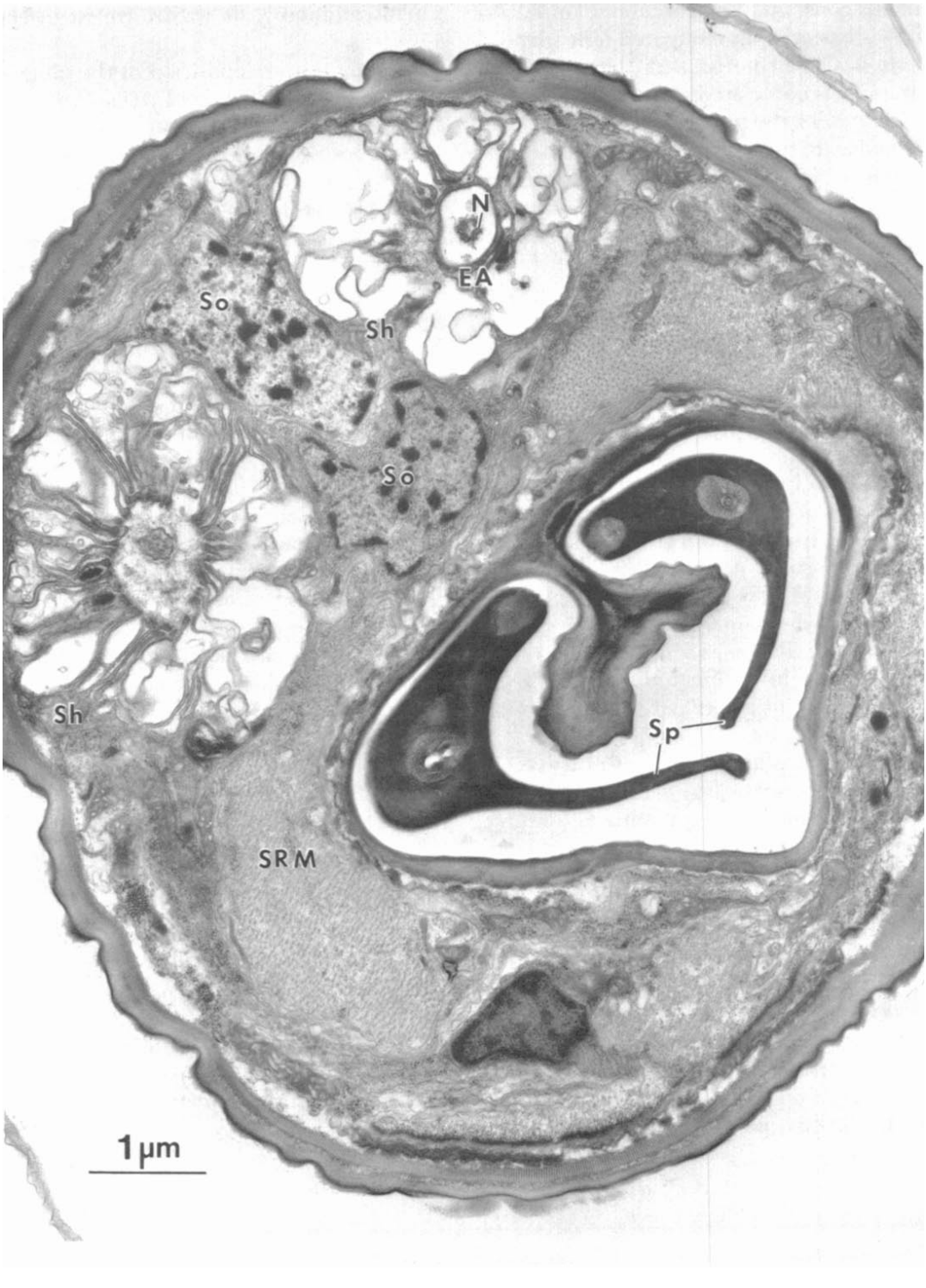

FIG. 12. *Meloidodera floridensis* young M5 cross section of phasmids. End apparatus (EA) visible around neuron (N) of right socket cell (So). Sp = spicules, SRM = spicule retractor muscle, Sh = sheath cell.

Socket cell and canal: The socket cell is better developed during the molt than intermolt. At molt the transient lamellar membranes provide secretory precursors to the cuticle lining of the canal.

Cuticular components such as acid mucopolysaccharides (glycosaminoglycans) have been histochemically detected in phasmids (33), and chondroitin sulfate and hyaluronic acid are both components which support collagen in the nematode cuticle (26). During formation of the canal in the prehatch J2, socket cell membranes infused with an electron-dense material accumulate at the outer edge of the canal region. When each stage is fully developed, occasional dark deposits appear along the outer edge of the cuticular canal. This could be a remnant of the earlier dark membrane secretion, observed during molt, which had not become modified into the hyaline state of the canal lining.

The content of phasmid secretions may vary with developmental time. It would not be surprising to see a large proportion of cuticle precursors in the premolt secretion being followed by increasing amounts of lipid before hatch or ecdysis. This is the case in dermal wax gland cells in insects which have alternate layering of cuticle and a wax complex (46).

Lamellae at the base of the sheath cell receptor cavity appear to form part of the end apparatus of the canal within the receptor cavity. A possible parallel is seen in insects where the end apparatus also appears to be constructed by the gland cell in class-3 epidermal glands (34,46).

During the middle molt of *M. floridensis* M4, and probably during other stages, microtubules are scattered in the socket cell. The surrounding cells and cuticle are reforming at this time, and these long tubules may be especially important for cellular support and morphological polarity during development (11). Regular arrays of microtubules (11) are not seen in the stages between molts in *Meloidodera* as they are in *Heterodera* J2 (1).

The presence of two socket cells in J2 and M5 phasmids of *Meloidodera* versus only one socket cell in *Heterodera* (1) may be a function of the relatively large canal in *Meloidodera* rather than an independent phylogenetic character. *Caenorhabditis elegans* J1 have only hypodermis for this function, J2 have one socket cell, and males have two socket cells associated with a long canal (44).

Neuron: The neuron represents the most continuous structure of the phasmid throughout all stages, although its morphology varies during development.

Only one ciliary dendrite is observed in all developmental stages of *Meloidodera* phasmids, as in *H. schachtii* (1), and adult *Scutellonema brachyurum* (47). Two neurons occur in phasmids of the animal parasites *Dracunculus medinensis* (33) and *Dipetalonema viteae* (31) and the free-living nematode *C. elegans* (44).

In *Meloidodera* the dendrite terminates in the receptor cavity between molts and in the adult, but it has an extensive distal zone and extends into the canal during the molt. The direction of development is from a complete to a shortened dendrite.

Vacuoles in the enlarged dendrite base of *Meloidodera* males are more apparent in stages after the molt than during the molt, and a true basal body might be present only during the middle of the molt when rootlets are present. The rarity of finding rootlets and basal bodies in this and other studies of sensory neurons supports the notion of their rapid disappearance associated with vacuolization and aging.

A small portion of the canal completely encircles the dendrite in the early M5; however, this part of the canal is shorter than its counterpart in other nematodes (24,31). Therefore, for some other nematodes the possible character state of neuron in the canal would not apply to the fully developed stages of *Meloidodera*.

Morphological differences of the neuron, such as degree of vacuolization, apparent shortening of the distal segment, and position relative to the canal, may have functional significance. For example, a shortened dendrite that ended in the receptor cavity rather than in the canal was

the only morphological aberration in *Caenorhabditis* OSM3 FITC staining mutants. While unable to detect salt and dauer pheromone, the mutant neurons could still detect carbon dioxide (37). Carbon dioxide is an important signal for hatching and molting (39). Thus it is conceivable that during the intermolt these shortened neurons respond primarily to a molting stimulus.

Neuron function might also be associated with its relative position in the channel. The chemical microenvironment surrounding the distal cilium could be different in the receptor cavity or the canal. In insects, the end apparatus and duct are believed to be physiological compartments containing enzymes such as esterase for extracellular reactions in the final stage of secretion from the epidermal glands (34). Physiological compartmentalization is suggested in these results by the more condensed secretion near the end apparatus and the near absence of secretion in the canal in intermolt stages.

Changes in length and position of the dendrite observed in these studies also occur at the beginning of the molt in insects under the control of ecdysone. Although this insect dendrite responds to stimulation, its response amplitude is probably different from its amplitude during the fully developed stage. This changed amplitude could be a compensation for the loss, during molt, of the transepithelial potential from the microvilli of the tormogen cell surrounding the receptor cavity (16).

If the presence or absence of dendrites in the canal proves to be a variable character within the Heteroderinae or higher taxa, this direction of development could support the absence of dendrites in the canal in adult males as a derived state. Lacking a precise knowledge of function, we are unable to identify possible selection pressures for homoplasy (i.e., parallel evolution). We have noted that the dendrite appears to lose its distal region through vesiculation as in chemosensory organs of certain insects (52). This pattern of neuron loss may prove to be present in all molt to intermolt transitions in plant parasites. Thus the absence of the dendrite in the canal may be directly related to some parasitic function, rather than to a relatively stable phylogenetic ancestry.

Sheath cell: The most outstanding features of the sheath cells of *Meloidodera* phasmids are the extensive infolded lamellae of the plasma membrane. These are not reported in the sheath cell around the phasmid neuron of *Caenorhabditis* (44). In *M. floridensis* a few lamellae occur in the anterior counterpart to the phasmid, called the amphid (unpubl.). However, only after host infection do amphids develop extensive lamellae or reticulations in *Heterodera* (23). Although lamellae are not found in lateral and caudal epidermal glands of most Adenophorea, extensive lamellae do occur in the lateral bacillary bands of the adenophorean animal parasitic trichurids, and they are believed to be osmotically important (51). Lamellae are also found in only one of the three neurons of the spicules of *Meloidodera, Verutus,* and *Heterodera* (unpubl.). This suggests that highly developed lamellae may serve some function in addition to protection of the neuron. Some idea of this lamellar function might be gained from associations in other systems. Extensive lamellae of similar proportions to the sheath cell of *Meloidodera* phasmids are visible in the salt receptors of the blowfly (25), salt glands of various other organisms (7,10,13), and mosquito rectal glands (32).

Because similar fixation techniques were used, the variations in degree of inflation of lamellar membranes in this work appear to reflect developmental differences; however, osmotic effects can influence the inflation. Hypertonic solutions caused extreme interlamellar inflation in *Scutellonema* (47). Therefore special care must be taken in the comparative morphology of phasmid sheath cells to standardize fixation procedures.

Lamellar membranes in *Meloidodera* are highly labile from the end of the molt to

the completion of a given stage. Particularly at the end of the molt, their relative dimensions and shapes may prove to be species specific. For instance, large distal lamellar anastomoses, relatively thick lamellae, and deep oval pockets are distinctive features of sheath membranes in *M. charis*. Use of sheath cell membrane patterns as a potential phylogenetic character requires observations of a number of specimens under precisely defined conditions and life stages.

Some unusual organelles are observed in sheath cells of *Meloidodera*. These include multivesicular bodies, multilamellar bodies, and membrane-filled vesicles. Multivesicular bodies were described in *Dipetalonema* phasmids (31). Very similar organelles have been seen in a hypodermal sensory organ of *Chromadorina germanica* (Adenophorea) (27), in rectal glands of *Meloidogyne javanica* (4), in the intestine of *Ascaris* (41), in salt glands of invertebrates and plants (10), and in insect dermal glands (34). Membrane-filled vesicles are present in lateral hypodermal cells of *Heterodera* (50). Many studies suggest a lysosomal function for these organelles (10,14); in some cases, however, these bodies are so numerous it suggests a secretory function (34). Multivesicular bodies are present when Golgi bodies are absent and might concentrate and sequester protein as Golgi analogues (27).

Observations in *Meloidodera* phasmids lend support to the proposed secretory and Golgi-like nature of these multivesicular bodies. Because of their similar shape to the concentric lamellar membranes in prehatch cells, multivesicular and multilamellar bodies may represent the remnants of lamellar membranes that did not reach the extracellular boundary of the receptor cavity. The lamellar membranes that did reach the receptor cavity showed distinctive Golgi-like behavior in their vesiculation at both ends. However, the possible origin of concentric lamellae within the nucleus rather than surrounding it makes a true Golgi assignment questionable.

Part of the source of the lamellar membranes appears to be the extensive hyaline lipid associated with socket cell nuclei before hatch. During the molts of later intermediate stages an electron-dense body in the socket cell may represent another form of lipid for the membranes which reappear at the end of the molt.

Sheath cell lamellae are numerous during the second half of the molt (J1 and J2) but are absent during the beginning of the molt (M3 through M5). Therefore they appear to be in a cycle of degeneration between molts. This is borne out by the apparent loss of much membrane material from prehatch to posthatch J2. Beyond the J2, lamellae become less numerous in successive intermolt stages as well, perhaps because of decreasing lipid in these nonfeeding stages. The sheath cell in the M5 has considerably less membrane area than in any juvenile.

Loss of lamellae at molt, and lamellar reduction in M3 and M4, may be functionally associated with the general muscular atrophy and inactivity at these developmental times. A well-developed osmotic detection ability, perhaps represented by these lamellae, may be more important to active than inactive stages. It was reported that secernentean nematodes with high turgor pressure in a terrestrial environment had phasmids, whereas low turgor pressure marine nematodes lacked phasmids (36).

We have only begun to evaluate the phylogenetic consequences of the different phasmid structures. Even tentative conclusions regarding these features must wait for observations on additional members of the Heteroderinae and its putative phylogenetic outgroup, the Hoplolaimidae (3). These observations, however, provide some understanding of the degree of morphological and fine structural variations which are possible complexities of phasmids, as well as speculations on function which may contribute to phylogeny. In light of the reports of phasmid disappearance in other genera (8), it is significant that the phasmid

of *Meloidodera* is never completely lost during any stage.

Literature Cited

1. Baldwin, J. G. 1985. Fine structure of the phasmid of second stage juveniles of *Heterodera schachtii*. Canadian Journal of Zoology 63:534–542.
2. Baldwin, J. G. 1986. Testing hypotheses of phylogeny of Heteroderidae. Pp. 75–100 *in* F. Lamberti and C. E. Taylor, eds. Cyst nematodes. New York: Plenum Publishing Co.
3. Baldwin, J, G., and L. P. Schouest, Jr. 1990. Comparative detailed morphology of the Heteroderinae Filip'ev & Schuurmans Stekhoven, 1941, sensu Luc et al. (1988): Phylogenetic systematics and revised classification. Systematic Parasitology 15:81–106.
4. Bird, A. F. 1971. The structure of nematodes. New York: Academic Press.
5. Bird, A. F. 1979. Ultrastructure of the tail region of the second stage preparasitic larva of the root knot nematode. International Journal of Parasitology 9:357–370.
6. Byard, E. H., W. J. Sigurdson, and R. A. Woods. 1986. A hot aldehyde-peroxide fixation method for electron microscopy of the free-living nematode *Caenorhabditis elegans*. Stain Technology 61:33–38.
7. Carr, K. E., and P. G. Toner, editors. 1982. Cell structure: An introduction to biomedical electron microscopy, 3rd ed. New York: Churchill Livingstone.
8. Carta, L. K., and J. G. Baldwin. 1990. Phylogenetic implications of phasmid absence in males of three genera of Heteroderinae. Journal of Nematology 22:386–394.
9. Coomans, A., and A. DeGrisse. 1981. Sensory structures. Pp. 127–174 *in* B. M. Zuckerman and R. A. Rohde, eds. Plant parasitic nematodes, vol. 3 New York: Academic Press.
10. Copeland, D. E., and A. T. Fitzjarrell. 1968. The salt absorbing cells in the gills of the blue crab (*Callinectes sapidus* Rathbun) with notes on modified mitochondria. Zeitschrift für Zellforschung und Mikroskopische Anatomie 92:1–22.
11. Dustin, P. 1978. Microtubules. New York: Springer-Verlag.
12. Eisenback, J. D. 1985. Techniques for preparing nematodes for scanning electron microscopy. Pp. 79–105 *in* K. R. Barker, C. C. Carter, and J. N. Sasser, eds. An advanced treatise on *Meloidogyne*, vol. 2. Methodology. Raleigh: North Carolina State University Graphics.
13. Eisenbeis, G., and W. Wichard. 1977. Zur feinstrukturellen Anpassung des Transportepithels am Ventraltubus von Collembolen bei unterschiedlicher Salinität. Zoomorphologie 88:175–188.
14. Ferris, V. R. 1979. Cladistic approaches in the study of soil and plant parasitic nematodes. American Zoologist 19:1195–1215.
15. Ferris, V. R. 1985. Evolution and biogeography of cyst-forming nematodes. European and Mediterranean Plant Protection Organization Bulletin 15:123–129.
16. Gnatzy, W., and F. Romer. 1980. Morphogenesis of mechanoreceptor and epidermal cells of crickets during the last instar, and its relation to molting-hormone level. Cell Tissue Research 213:369–391.
17. Hartman, K. M. 1978. The biology, host range and occurrence of *Meloidodera charis* in Arizona. M.S. thesis, University of Arizona, Tucson.
18. Hawke, S. D., and R. D. Farley. 1971. The role of pore structures in the selective permeability of antennal sensilla of the desert burrowing cockroach, *Arenivaga* sp. Tissue and Cell 3:665–674.
19. Hedgecock, E. M., J. G. Culotti, J. N. Thomson, and L. A. Perkins. 1985. Axonal guidance mutants of *Caenorhabditis elegans* identified by filling sensory neurons with fluorescein dyes. Developmental Biology 111:158–170.
20. Herman, R. 1984. Analysis of genetic mosaics of the nematode *Caenorhabditis elegans*. Genetics 108: 165–180.
21. Hirschmann, H., and A. C. Triantaphyllou. 1973. Postembryogenesis of *Meloidodera floridensis* with emphasis on the development of the male. Journal of Nematology 5:185–195.
22. Hubel, D. H. 1957. Tungsten microelectrode for recording from single units. Science 125:549–550.
23. Jones, G. M. 1979. The development of amphids and amphidial glands in adult *Syngamus trachea* (Nematoda: Syngamidae). Journal of Morphology 160: 299–322.
24. Kozek, W. J., and T. C. Orihel. 1983. Ultrastructure of *Loa loa* microfilaria. International Journal of Parasitology 13:19–43.
25. Larsen, J. R. 1962. The fine structure of the labellar chemosensory hairs of the blowfly, *Phormia regina* Meig. Journal of Insect Physiology 8:683–691.
26. Lee, D. L. 1977. Physiology of nematodes, 2nd ed. New York: Columbia University Press.
27. Lippens, P. L. 1974. Ultrastructure of a marine nematode, *Chromadorina germanica* (Buetschli, 1874). II. Cytology of lateral epidermal glands and associated neurocytes. Zeitschrift für Morphologie der Tiere 79:283–294.
28. Locke, M. 1961. Pore canals and related structures in insect cuticle. Journal of Biophysical and Biochemical Cytology 10:589–619.
29. Locke, M. 1974. The structure and formation of the integument in insects. Pp. 123–213 *in* M. Rockstein, ed. The physiology of Insecta, vol. 6, 2nd ed. New York: Academic Press.
30. Luc, M., A. R. Maggenti, and R. Fortuner. 1988. A reappraisal of Tylenchina (Nemata). 9. The family Heteroderidae Filip'ev & Schuurmans Stekhoven, 1941. Revue de Nématologie 11:159–176.
31. McLaren, D. J. 1976. Nematode sense organs. Pp. 195–265 *in* B. Dawes, ed. Advances in parasitology, vol. 14. New York: Academic Press.
32. Meredith, J., and J. E. Phillips. 1973. Rectal ultrastructure in salt and freshwater mosquito larvae in relation to physiological state. Zeitschrift für Zellforschung und Mikroskopische Anatomie 138:1–22.
33. Muller, R., and D. S. Ellis. 1973. Studies on

Dracunculus medinensis (Linnaeus). III. Structure of the phasmids in the first-stage larva. Journal of Helminthology 47:27–33.

34. Noirot, C., and A. Quennedey. 1974. Fine structure of insect epidermal glands. Annual review of Entomology 19:61–80.

35. Othman, A. A. 1985. Comparison of characters with SEM for systematics and phylogeny of Heteroderidae (Nematoda: Tylenchida). Ph.D thesis, University of California, Riverside.

36. Paramonov, A. A. 1954. On the structure and function of the phasmids. Trudy Gelmintologicheskaya Lab Akademiya Nauk SSR 7:19–49.

37. Perkins, L. A., E. M. Hedgecock, J. N. Thomson, and J. G. Culotti. 1986. Mutant sensory cilia in the nematode *Caenorhabditis elegans*. Developmental Biology 117:456–487.

38. Porter, K. R., and M. A. Bonneville. 1973. Fine structure of cells and tissues, 4th ed. Philadelphia: Lea and Febiger.

39. Rogers, W. P., and T. Petronijevic. 1982. The infective stage and the development of nematodes. Pp. 3–28 *in* L. E. A. Symons, A. D. Donald, and J. K. Dineen, eds. Biology and control of endoparasites. New York: Academic Press.

40. Schafer, R., and T. V. Sanchez. 1976. The nature and development of sex attractant specificity in cockroaches of the genus *Periplaneta*. Journal of Morphology 149:139–158.

41. Sheffield, H. G. 1964. Electron microscope studies on the intestinal epithelium of *Ascaris suum*. Journal of Parasitology 50:365–379.

42. Siddiqi, M. R. 1978. The unusual position of the phasmid of *Coslenchus costatus* and other Tylenchidae. Nematologica 24:449–455.

43. Singh, R. N., and J. E. Sulston. 1978. Some observations on moulting in *Caenorhabditis elegans*. Nematologica 24:63–71.

44. Sulston, J. E., D. G. Albertson, and J. N. Thomson. 1980. The *Caenorhabditis elegans* male: Postembryonic development of nongonadal structures. Developmental Biology 78:542–576.

45. Triantaphyllou, A. C., and H. Hirschmann. 1973. Environmentally controlled sex expression in *Meloidodera floridensis*. Journal of Nematology 5:181–185.

46. Waku, Y. 1982. Fine structure of the insect wax glands. Pp. 113–116 *in* H. Akai, R. C. King, and S. Morohoshi, eds. The ultrastructure and functioning of insect cells. The Society for Insect Cells, Tokyo.

47. Wang, K. C., and T. A. Chen. 1985. Ultrastructure of the phasmids of *Scutellonema brachyurum*. Journal of Nematology 17:175–186.

48. White, J. G., E. Southgate, J. N. Thomson, and S. Brenner. 1986. The structure of the nervous system of the nematode *Caenorhabditis elegans*. Philosophical Translations of the Royal Society of London Biological Sciences 314:1–340.

49. Wigglesworth, V. B. 1976. The distribution of lipid in the cuticle of *Rhodnius*. Pp. 89–106 *in* H. R. Hepburn, ed. The insect integument. New York: Elsevier Publishing Co.

50. Wisse, E., and W. Th. Daems. 1968. Electron microscopic observations on second stage larvae of the potato root eelworm *Heterodera rostochiensis*. Journal of Ultrastructure Research 24:210–231.

51. Wright, K. A. 1980. Nematode sense organs. Pp. 237–295 *in* B. M. Zuckerman, ed. Nematodes as biological models, vol. 2. New York: Academic Press.

52. Zacharuk, R. Y. 1980. Ultrastructure and function of insect chemosensilla. Annual Review of Entomology 25:27–47.

53. Zuckerman, B. M., and H.-B. Jansson. 1984. Nematode chemotaxis and possible mechanisms of host/prey recognition. Annual Review of Phytopathology 22:95–113.